doi:10.55385/kastamonujes.1570731 KUJES 10(2):94-103, 2024

Kastamonu University
Journal of Engineering and Sciences
e-ISSN 2667-8209
http://dergipark.gov.tr/kastamonujes

Preparation and Properties of Foamable Ni-GNP/AlSi12 Precursor Materials

Kilani A. Mohamed Hassan[a], **Arif Uzun**[b,*]

[a] Department of Materials Science and Engineering, Institute of Science, Kastamonu University, Kastamonu, Türkiye
[b] Department of Mechanical Engineering, Kastamonu University, Kastamonu, Türkiye
***Corresponding Author:** auzun@kastamonu.edu.tr

Received: **October 20, 2024** ◆ Accepted: **December 20, 2024** ◆ Published Online: **December 25, 2024**

Abstract: In this study, nickel-coated graphene nanoplatelets reinforced AlSi12 precursor materials were produced by powder metallurgy method. For this process, Ni-GNP particles were added to the matrix material AlSi12 powders at different ratios (0%, 0.4%, 0.8% and 1.2% by weight). Then, the mixed powders were cold compressed and extruded at different ratios, and foamable precursor samples with diameters of 6 and 12 mm were produced. Microstructural analyses, density measurements and microhardness tests were carried out to evaluate the effects of Ni-GNPs on the properties of foamable precursor materials. Microstructure and surface analysis of Ni-GNP/AlSi12 precursor materials showed high density, uniform distribution of Ni, localized Si phases and surface oxidation due to reactivity of aluminum. It was revealed that the addition of Ni-GNP led to the formation of Al-Ni intermetallic phases, reduced the Al peak intensity and strengthened the graphene bond with the Al matrix. The relative density increased with increasing extrusion ratio, higher Ni-GNP content decreased the relative density but improved it significantly after extrusion. The maximum hardness was achieved in the precursor materials with the optimum graphene content of 0.4 wt%, while higher amounts led to aggregation, increased porosity and decreased hardness.

Keywords: AlSi12, Ni-GNP, powder metallurgy, microstructure analysis

Öz: Bu çalışmada toz metalurjisi yöntemi ile nikel kaplı grafen nanoplakçıklar ile takviyelendirilmiş AlSi12 öncü malzemeler üretilmiştir. Bu işlem için farklı oranlarda (ağırlıkça %0, %0.4, %0.8 ve %1.2) Ni-GNP parçacıkları matris malzemesi AlSi12 tozlarına ilave edilmiştir. Akabinde karışım tozlar soğuk olarak sıkıştırılmış ve farklı oranlarda ekstrüzyon işlemine tabi tutulmuş ve 6 ve 12 mm çaplara sahip köpürebilir öncü numuneler üretilmiştir. Ni-GNP'lerin köpürebilir öncü malzemelerin özellikleri üzerindeki etkilerini değerlendirmek için mikro yapısal analizler, yoğunluk ölçümleri ve mikro sertlik testleri gerçekleştirildi. Ni-GNP/AlSi12 öncü malzemelerin mikro yapısı ve yüzey analizi, yüksek yoğunluk, Ni'nin düzgün dağılımı, lokalize Si fazları ve alüminyumun reaktifliğinden dolayı yüzey oksidasyonunu gösterdi. Ni-GNP eklenmesinin Al-Ni intermetalik fazların oluşumuna yol açtığını, Al pik yoğunluğunu azalttığını ve grafen bağını Al matrisiyle güçlendirdiğini ortaya koydu. Artan ekstrüzyon oranı ile birlikte bağıl yoğunluk artmış, daha yüksek Ni-GNP içeriği bağıl yoğunluğu azaltmış ancak ekstrüzyondan sonra önemli ölçüde iyileştirmiştir. Optimum grafen içeriğinin %0,4 ağırlıkta olmasıyla öncü malzemelerde maksimum sertlik elde edilirken, daha yüksek miktarlar kümeleşmeye, gözenekliliğin artmasına ve sertliğin azalmasına yol açmıştır.

Anahtar Kelimeler: AlSi12, Ni-GNP, toz metalurjisi, mikroyapı analizi

1. Introduction

The production of aluminium foam by powder metallurgy starts with the mixing of starting powders, compaction of the powders and secondary processes such as rolling or extrusion. The materials produced after these process are called foamable materials. Therefore, foamable materials have an important place in aluminium foam production. The reason for this is that the physical and mechanical properties of foamable materials affect the properties of the foam structure. For example, low density foamable material produced by powder metallurgy method can exhibit lower expansion when subjected to foaming process. In this case, the density of the foam produced is high [1].

Melting methods, especially powder metallurgy, are used extensively in aluminium foam production [2-4]. In addition, there are many methods developed by researchers [5]. Foam production from foamable materials is mainly included in the powder metallurgy process. The mechanical and physical properties of foams do not only depend on the mechanical and physical properties of the foamable material. In fact, the chemical composition of the structure of the foamable material can also affect the properties of the final product, aluminium foam. In this respect, various ceramic reinforcements are suggested for the improvement of mechanical properties of aluminum foams. Especially the effects of nanoparticles have become a focus of research topics. Papantoniou and Manolakos [6] investigated the production and characterization of aluminum foam reinforced with nanostructured γ-Al_2O_3 using AA5083 plates. Foamable materials were produced by incorporating TiH_2 and γ-Al_2O_3 particles by friction stirring process and then foamed in a laboratory

oven. The researchers achieved a mean porosity of 70% and a plateau stress of 27 MPa in the foam structure they obtained. Wang et al. [7] used high energy ball milling (HEBM) and powder metallurgy techniques for the production of carbon nanotube (CNT) reinforced closed cell Al-Si composite foams. The starting powders for the production of Al-Si foams containing different CNT ratios (0.25%, 0.5% and 0.75%) were compressed under 500 MPa pressure and foamable materials were produced. It was determined that the inclusion of 0.50 wt% CNTs in the composite foams produced after foaming increased the fatigue strength by 54% compared to Al-Si foams, since it reduced the crack expansion rates and changed the failure modes. On the other hand, another study conducted by the researchers emphasized that CNT content can reduce the pore size and improve circularity. In particular, CNTs/Al composite foams with 1.0 wt% exhibited optimum compressive properties [8]. Gao et al. [9] observed improvement in mechanical properties by incorporating copper-coated carbon fibers (Cf) into aluminum foam. The researchers investigated the effect of Cf on bubble nucleation, growth, and foam stability in aluminum sandwich foams. In the study, the foamable interlayer was produced by powder metallurgy and rolling processes to form the sandwich structure before foaming. Pang et al. [10] produced foamable precursors using TiH_2 and Al_2O_3 powders with 7075 aluminum plates by friction stir process. Their analysis revealed that the rotation speed significantly affected the uniformity and density of precursors, while the welding speed had minimal effect. Rathore et al. [11] used an underwater method for friction mixing process which allows better mixing of foaming agent and stabilizer into the substrate for foamable precursor production.

Comprehensive research has been conducted on the production of aluminum foam with foamable precursor materials and the characterization of the produced foams. However, it has been observed that sufficient studies have not been conducted on the properties of foamable precursor materials. The produced foamable precursor materials are essentially a type of composite material. In our current research, Ni-coated GNP particles were selected as the reinforcement phase in the preparation of foamable AlSi12 materials by powder metallurgy method. The effect of Ni-GNP particles added to the AlSi12 matrix as reinforcement phase at different ratios on the physical properties and hardness changes of Ni-GNP/AlSi12 precursor materials was analyzed.

2. Experimantal procedures

2.1. Materials

In experimental studies, Al powder (99.8% pure - < 44 μm-round shaped) as matrix material from Buha powder company, Si powder (< 44 μm-sharp cornered) as alloying element from Acros Organics, TiH_2 powder (< 44 μm-sharp cornered) as foaming agent from Sigma Aldrich company and graphene nanoplatelets (GNPs) (99.9% purity - 3 nm size) as reinforcement element from Nanografi company were obtained. Figure 1 shows the scanning electron microscope (SEM) images of the powders used in the experimental study.

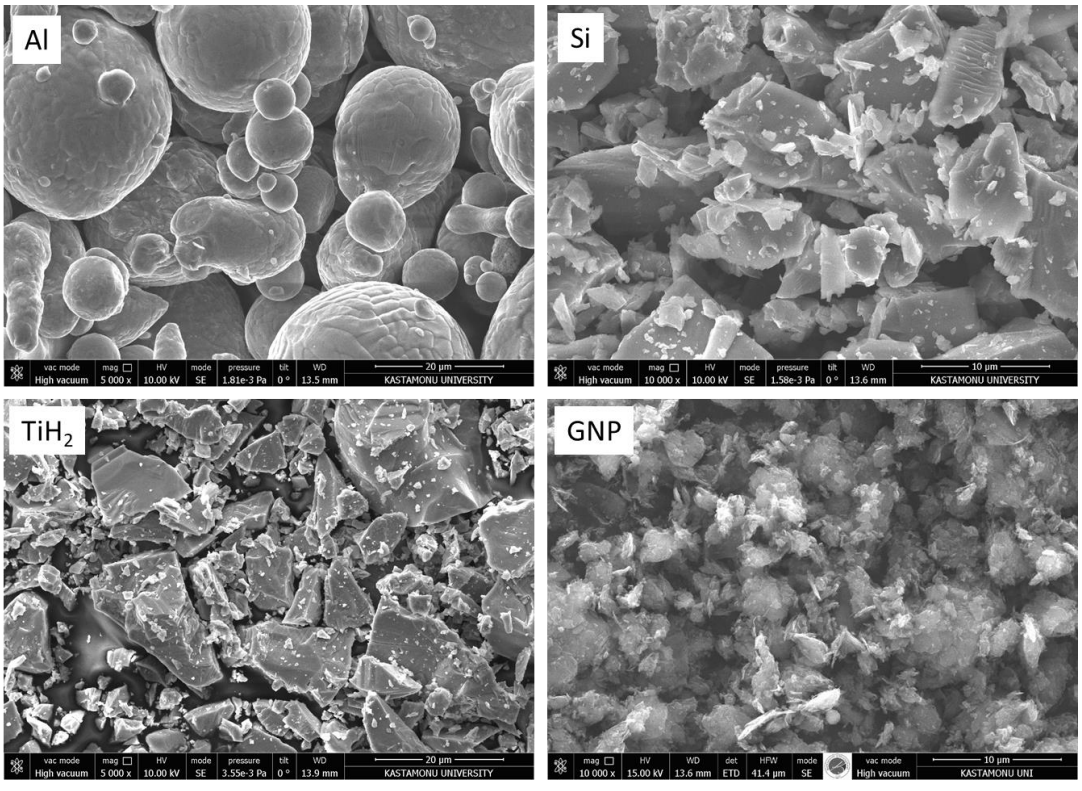

Figure 1. SEM images of the powders used in the experimental study

The chemical method was used for coating the GNPs with nickel. Sodium hydroxide (NaOH - 96%), nitric acid (HNO_3 - 68%), hydrochloric acid (HCl - 37.5%), tin(II) chloride (SnCl2 - 99%), tin (Sn - 99.5%), silver nitrate ($AgNO_3$ - 99.8%), ammonium hydroxide solution (28% NH_3. H_2O), nickel sulfate hexahydrate $NiSO_4 \cdot 6H_2O$ - 98.0%), ammonium chloride (NH_4Cl - 99.5%), disodium hydrogen citrate sesquihydrate ($Na_2HC_6H_5O_7 \cdot 1.5H_2O$ - 98.0%), boric acid (H_3BO_3 - 99.5%), sodium hypophosphite (NaH_2PO_2 - 99.0%) and distilled water were used in the preparation [12].

2.2. Production of Ni-GNP/AlSi12 Precursor Materials

GNPs were chemically coated with Ni before the production of Ni-GNP/AlSi12 precursor materials. The preparation of the Ni-coated GNPs consisted of five steps: (i) the GNPs were cleaned, (ii) the surfaces of the GNPs were roughened, (iii) the GNPs were sensitized, (iv) the GNPs were activated and in the final step (v) the coating process was carried out. After coating, experimental work continued by mixing the initial powders in a planetary ball milling device (PM-100, Retsch, Germany). For this process, 0 wt%, 0.4 wt%, 0.8 wt% and 1.2 wt% Ni coated GNPs, 1 wt% TiH_2 as foaming agent and 12 wt% Si as alloying element were added to the aluminum powders and mixed in a stainless steel container with a ball mixer for 60 minutes. Stainless steel balls with a diameter of 8 mm were added to the powder mixture to achieve a ball to powder ratio of 5:1 by weight. 0.3% stearic acid was added to the mixture to ensure effective dispersion of Ni coated GNPs, to prevent adhesion of the powders to the vessel walls and balls and to minimize the cold welding effect of the powder particles.

The mixed powders were compacted unidirectional in a steel mold under 600 MPa pressure using a hydraulic press. After compression, cylindrical billets with a diameter of 27 mm were produced (Fig. 2a) and these were placed in a steel mold and kept in an oven at 430ºC for 3 hours. Afterwards, the mold was removed from the oven and placed on a steel unit integrated into a vertical hydraulic press unit and extrusion process was carried out. The billets were extruded at two different extrusion ratios (1:5 and 1:20) to produce Ni-GNP/AlSi12 precursor samples with diameters of 6 mm and 12 mm (Fig. 2b).

Figure 2. Compressed block sample (billet) (a) and extruded Ne-GNP/AlSi12 precursor samples

2.3. Characterization

The densities (ρ_s) of Ni-GNP/AlSi12 precursor materials and Ni-GNP/AlSi12 foams were measured according to the archiment principle using a density kit integrated in a balance with a precision of 0.0001 g. The formula given in Equation 1 was used in the calculations.

$$\rho_s = \frac{m_{s_{air}}}{\left(m_{s_{air}} - m_{s_{water}}\right)} \times \rho_{water} \quad (1)$$

Where ρ_s is the density of the sample, ρ_{water} is the density of water at room temperature, $m_{s_{air}}$ is the weight of the sample in air and $m_{s_{water}}$ is the weight of the sample in water.

The theoretical densities (ρ_t) of the samples were calculated according to the mixing rule. Relative density (ρ*) values were obtained as the ratio of the experimental density to the theoretical density (Equation 2).

$$\rho * = {}^{\rho_s}/_{\rho_t} \times 100\% \quad (2)$$

Scanning electron microscopy (SEM) and integrated energy dispersive spectroscopy (EDS) were used for chemical composition and microstructural analysis of Ni-GNP/AlSi12 precursor materials. Metallographic evaluation of the prepared samples was carried out in a conventional way (grinding, polishing and etching). In addition, X-ray diffraction (XRD) device (Bruker) was used for phase determination. Measurements were performed in the range of 3 to 90 degrees and at a rate of 1.2 s/degree. The microhardness measurements of the Ni-GNP/AlSi12 precursor materials were performed on a Schimadzu (HMV-G) microhardness tester by applying a 300 g load for 10 seconds (HV0.3). The microhardness values were evaluated by averaging at least five measurements for each sample.

3. Result and Discussion

3.1. Microstructure of Ni-GNP/AlSi12 Precursor Materials

As seen in Figure 3, no obvious were observed in the microstructure photographs of the different composites. This indicates that the composites reached a high density after the extrusion process. On the surface of the composite materials with Ni-GNP addition, relatively black regions appeared. We think that these black regions are due to the condensation of Ni-GNPs as a result of agglomeration.

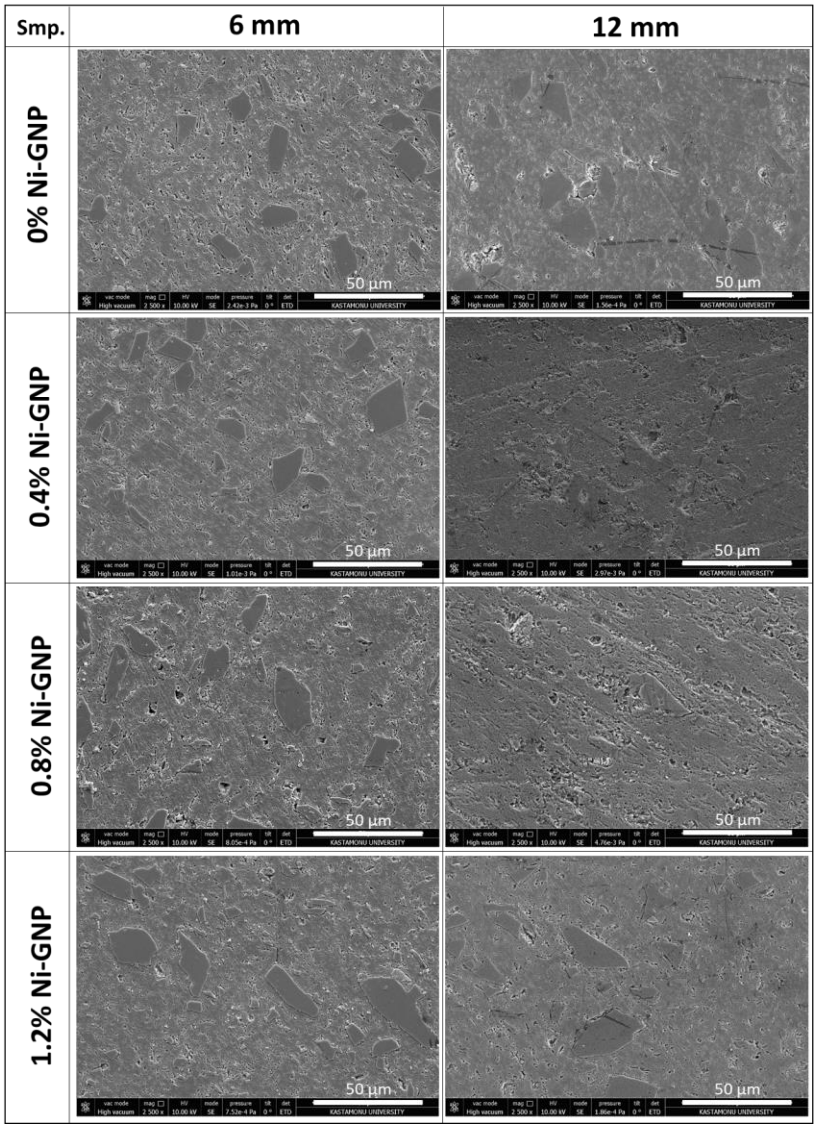

Figure 3. Microstructure photographs of Ni-GNP/AlSi12 precursor samples

Figure 4 shows the surface topography of the 1.2 wt% Ni-GNP/AlSi12 precursor material. The image reveals that the distribution of C and Ni elements in the EDS map of the composites is relatively uniform. Although the proportion of Ni is less than 1%, it is observed to be homogeneously distributed in the structure with a yellow color in the mapping. In addition, the formation of localized Si phases was observed on the sample surface. The green dots indicate the element O, indicating that oxidation has occurred on the surface of the composites. The cutting, polishing, characterization and other processes of the composites were carried out in the absence of atmospheric control. Therefore, oxidation became inevitable due to the tendency of aluminum to oxidize easily.

The interplay between a homogeneous Ni-GNP distribution and localized oxidation significantly affects the final properties of the material [13]. While the uniform distribution of Ni-GNPs enhances mechanical, thermal, and electrical properties, localized oxidation presents challenges that could limit performance. Addressing these challenges through material design and process optimization will unlock the full potential of the composite for advanced applications.

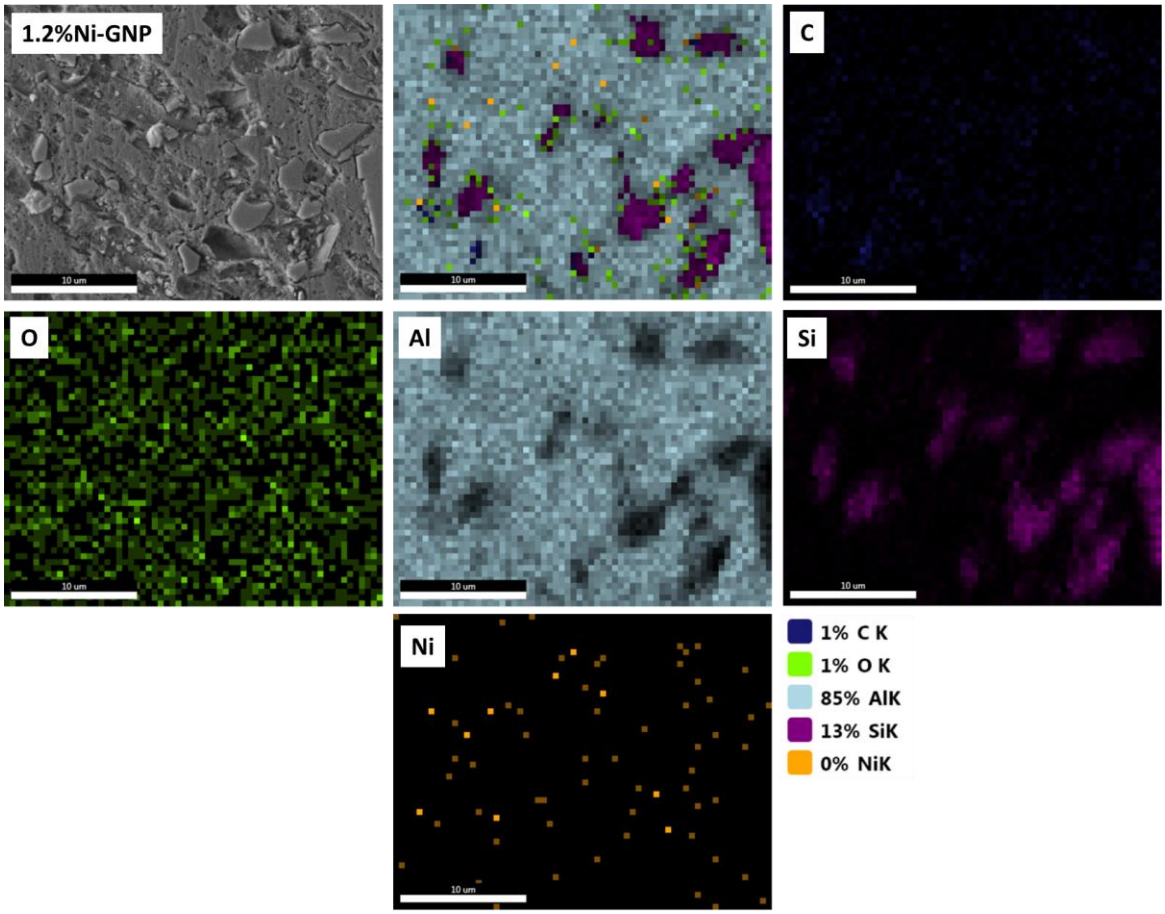

Figure 4. Surface topography and EDS map of the 1.2 wt% Ni-GNP/AlSi12 precursor material

3.2. XRD results

Figure 5 shows the XRD patterns of 0% Ni-GNP-AlSi12 and 2% Ni-GNP-AlSi12 samples. According to the XRD pattern of the 0% Ni-GNP-AlSi12 sample, Al (Bravais lattice: cubic, a = b = c = 4.040 nm) and Si (Bravais lattice: cubic, a = b = c = 5.430 nm) phases were detected. According to the XRD pattern of 2% Ni-GNP-AlSi12 sample, Al (Bravais lattice: cubic, a = b = c = 4.040 nm), Si (Bravais lattice: cubic, a = b = c = 5.420 nm), Al_3Ni_2 (Bravais lattice: hexagonal, a = 4.028; b = 4.028; c = 4.891 nm), Al_4Ni_3 (Bravais lattice: cubic, a = 11.480; b = 11.480; c = 11.480 nm) and C (Bravais lattice: hexagonal, a = 2.522; b = 2.522; c = 20.593 nm) phases were detected. The formation of Al_3Ni_2 and Al_4Ni_3 intermetallic between the Al matrix and the Ni coating demonstrates the effectiveness of nickel, which enables graphene to form a strong bond directly with the Al matrix. When the XRD patterns of 0% Ni-GNP and 2% Ni-GNP reinforced AlSi12 composites are compared, it is noticeable that the intensity of Al peaks decreases with the increase of graphene content. Al_3Ni_2 and Al_4Ni_3 phases are known to be brittle materials [14]. increase the strength of aluminum-based composites by acting as reinforcements within the matrix. These phases improve hardness and wear resistance, making the material suitable for high-load applications such as aerospace and automotive components.

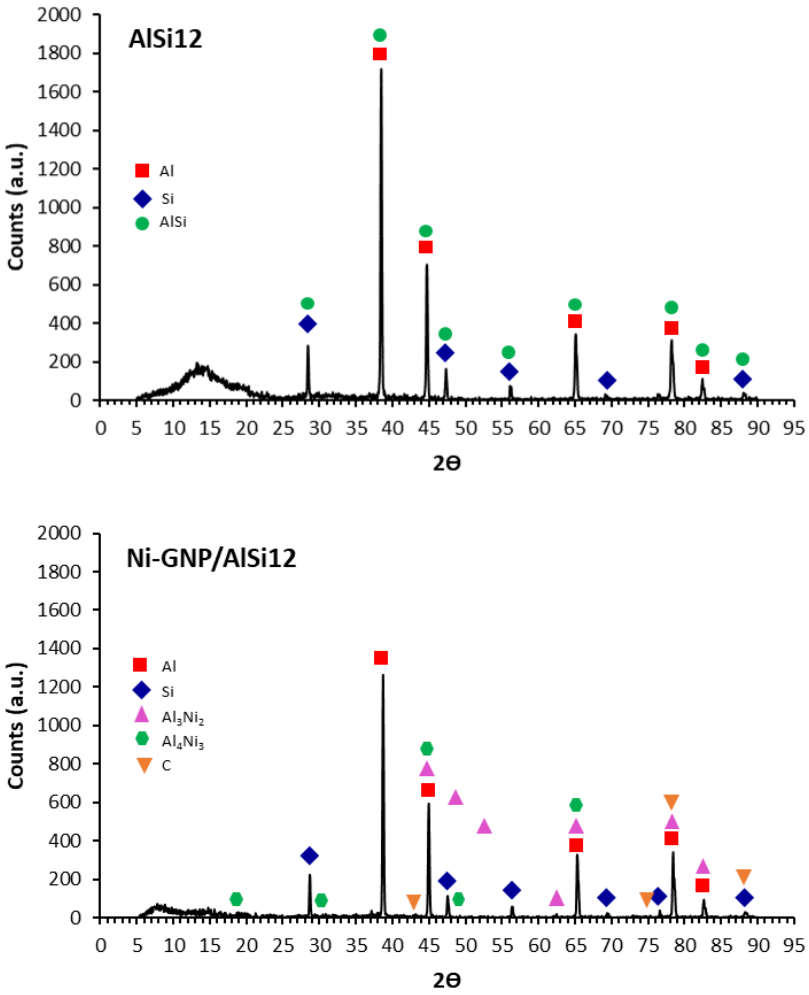

Figure 5. XRD patterns of 0% Ni-GNP-AlSi12 and 2% Ni-GNP-AlSi12 samples

3.3. Density Variation of Ni-GNP/AlSi12 Precursor Materials

In the production of Al-based composite materials, secondary processes such as extrusion, rolling and forging can be applied in addition to compression processes to obtain PM products with high density and low porosity [15]. However, the deformation that occurs in the preformed materials produced during these processes brings problems such as cracking. Abdel-Rahman and El-Sheikh [16] tried to explain the effect of relative density on the deformation properties of PM parts. According to the researchers, high stresses are needed for deformation of materials with high relative density.

Figure 6 shows the density change graph of Ni-GNP/AlSi12 precursor materials depending on secondary processing. The graph shows that the increase in the amount of particles decreases the relative density of the samples from 95.58% to 93.77% after pressing. On the other hand, this density difference of 1.81% decreased to 0.49% for samples with a diameter of 6 mm and 1.39% for samples with a diameter of 12 mm with extrusion. In both stages, the increase in the amount of Ni-GNP had a decreasing effect on the relative density of the samples. However, for the samples without Ni-GNP, the extrusion process increased the relative density value by 3.73% for the samples with a diameter of 6 mm and 3.55% for the samples with a diameter of 12 mm. With the increase in the amount of Ni-GNP (1.2%), this difference increased to 5.05% and 3.96%, respectively. Therefore, it can be said that extrusion processes increase the relative density values of foamable materials containing Ni-GNP.

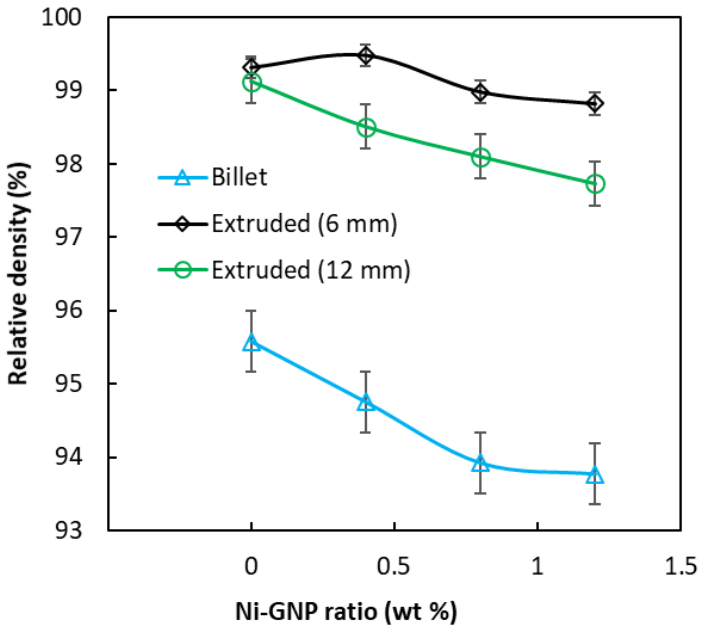

Figure 6. Density change of Ni-GNP/AlSi12 precursor materials

Table 1 shows the average density changes obtained in the samples as a result of the secondary processes applied. The increase in the deformation of the foamable materials due to the extrusion processes applied after the pressing process led to an increase in the relative density.

Table 1. Average density changes due to densification processes

Sample	Densification process	Density (g.cm^{-3})	Relative density (%)	Theoretical density (g.cm^{-3})
AlSi12	Billet	2.539	95.577	2.657
	Extruded (6 mm)	2.638	99.311	
	Extruded (12 mm)	2.633	99.123	
0.4% Ni-GNP/AlSi12	Billet	2.508	94.752	2.647
	Extruded (6 mm)	2.633	99.475	
	Extruded (12 mm)	2.607	98.504	
0.8% Ni-GNP/AlSi12	Billet	2.477	93.922	2.637
	Extruded (6 mm)	2.610	98.980	
	Extruded (12 mm)	2.587	98.097	
1.2% Ni-GNP/AlSi12	Billet	2.464	93.770	2.628
	Extruded (6 mm)	2.597	98.820	
	Extruded (12 mm)	2.568	97.728	

3.4. Hardness Changes of Ni-GNP/AlSi12 Precursor Materials

Graphene-reinforced aluminum composites exhibit improved stiffness compared to pure aluminum. Graphene, a two-dimensional allotrope of carbon, is known for its exceptional mechanical properties, including high strength and stiffness. Adding graphene to aluminum helps strengthen the composite by providing a reinforcing network within the metal matrix. If the graphene sheets are evenly distributed throughout the aluminum, they act as a barrier against dislocation movement and prevent deformation. This results in improved stiffness and resistance to plastic deformation [17, 18]. However, the specific relationship between the volume fraction of graphene nanolevels and the resulting hardness may vary depending on the composite system, production conditions and other factors. The effects of Ni-GNPs and extrusion rate on the hardness of aluminum composites are given in Figure 7. It is seen that the highest hardness values are obtained in the samples with a diameter of 6 mm for 0.4 wt% graphene content. However, it is seen that the specimens with a diameter

of 6 mm have higher hardness values compared to the specimens with a diameter of 12 mm. This is due to the fact that billet specimens with the same diameter are subjected to more plastic deformation. Thus, an increase in hardness is expected in denser specimens. The results show that the addition of GNPs up to 0.4 wt.% to pure aluminum increases the hardness of aluminum composites. The addition of graphene above 0.4 wt.% is thought to decrease the hardness of the composites due to the tendency of graphene to agglomerate. Therefore, the interaction between aluminum particles and GNPs is reduced by agglomeration. This leads to higher porosity and causes a decrease in hardness [19]. Studies highlight that excessive graphene content causes aggregation, leading to weaker interfacial bonds between the matrix and graphene particles [20]. Often, an optimum dispersion limit is formed, beyond which mechanical benefits are reduced due to poor stress transfer or pore formation [21].

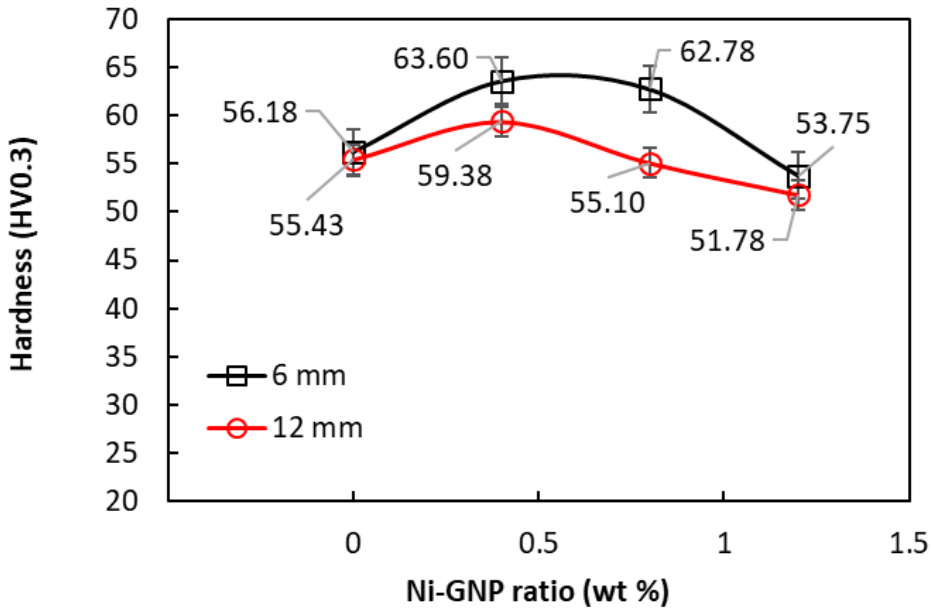

Figure 7. Hardness changes of Ni-GNP/AlSi12 precursor materials

4. Conclusion

It can be concluded that the addition of Ni-GNP to AlSi12 precursor materials significantly influences both the microstructure and mechanical properties of the composites. The microstructure analysis shows that the materials achieved high density after extrusion, with uniform distribution of Ni and C elements, although slight oxidation occurred on the surface. The presence of Ni-GNP contributed to the formation of intermetallic compounds (Al_3Ni_2, Al_4Ni_3) that strengthened the bond between graphene and the aluminum matrix, as demonstrated by the XRD analysis. The density of the composites was enhanced through secondary processes, such as extrusion, with Ni-GNP playing a key role in increasing the relative density, particularly in samples with higher Ni-GNP content. Additionally, the hardness of the composites was improved with the inclusion of graphene up to 0.4 wt.%, suggesting that the proper dispersion of graphene enhances the material's resistance to deformation. However, higher graphene concentrations resulted in agglomeration, leading to increased porosity and reduced hardness.

Ni-GNP/AlSi12 composites offer enhanced mechanical properties, particularly in terms of hardness and density, when optimal graphene content is maintained. However, controlling the dispersion of graphene is crucial to prevent negative effects like agglomeration, which can compromise the material's structural integrity. These findings highlight the potential of Ni-GNP as a reinforcing agent in aluminum composites, though further refinement in processing techniques may be needed to fully harness its benefits. Regarding industrial applications, the enhanced hardness and density of Ni-GNP/AlSi12 composites suggest their potential use in wear-resistant components, lightweight structural parts, and heat sinks in automotive and aerospace industries.

Conflict of Interest

All authors certify that they have no affiliations with or involvement in any organization or entity with any financial interest or non-financial interest in the subject matter or materials discussed in this manuscript.

Ethics Committee Approval

Ethics committee approval is not required.

Author Contribution

Conceptization: KMH, AU; methodology and laboratory analyzes: KMH, AU; writing draft: KMH, AU; supervisor : AU; proof reading and editing. All authors have read and agreed to the published version of manuscript.

Acknowledgements

Not appliable

5. References

[1]. Uzun, A., Asikuzun, E., Gokmen, U., Cinici, H., (2018). Vickers Microhardness Studies on B_4C Reinforced/Unreinforced Foamable Aluminium Composites. Transactions of the Indian Institute of Metals. 71:327-337.

[2]. Ding, X., Qian, H., Su, G., Hu, X., Liu, Y., Peng, G., Wu, Y., (2024). Reinforcement effect of fly ash with different morphologies on aluminum foam prepared via powder metallurgy. Powder Technology. 119944**.**

[3]. Zhiqiang, G., Yonglin, G., Guoyin, Z., Xiaoguang, Y., Feng, W., Jinwei, L., (2024). Foaming Behavior of AlMg4Si8 Matrix and Pure Al Matrix Precursors in Closed Cavities with Different TiH_2 Addition Levels. International Journal of Metalcasting. 1-16.

[4]. Yuan, G., Li, Y., Hu, L., Fu, W. (2023). Preparation of shaped aluminum foam parts by investment casting. Journal of Materials Processing Technology. 314:117897.

[5]. Kumar, M., Singh, R. K. R., Jain, V., (2023). Characterization of mechanical and metallurgical properties of AA6063 foam developed by friction stir precursor deposition technique. Journal of Adhesion Science and Technology, 37(18): 2608-2625.

[6]. Papantoniou, I. G., & Manolakos, D. E., (2024). Fabrication and characterization of aluminum foam reinforced with nanostructured γ-Al2O3 via friction stir process for enhanced mechanical performance. The International Journal of Advanced Manufacturing Technology. 130(11), 5359-5368.

[7]. Wang, S., Pu, B., Liu, G., Zhang, X., Sha, J., Zhao, N., Yang, X., (2024). Research on compression-compression fatigue properties of carbon nanotubes reinforced closed-cell aluminum matrix composite foams by reinforcement content design. Engineering Failure Analysis, 159:108117

[8]. Wang, S., Yang, K., Xie, M., Sha, J., Yang, X., Zhao, N. (2024). Effect of carbon nanotubes content on compressive properties and deformation behaviors of aluminum matrix composite foams. Materials Science and Engineering: A, 898:146391.

[9]. Gao, Q., Su, X., Feng, Z., Huang, P., Wei, Z., Sun, X., Zu, G. (2024). Preparation, bubbles evolution, and compressive mechanical properties of copper-coated carbon fibers/aluminum foam sandwich panels. Journal of Materials Research and Technology. 30:375-384.

[10]. Pang, Q., Wu, Z., Hu, Z., (2022). The influence of process parameters on the preparation of closed-cell aluminum foam by friction stir processing. The International Journal of Advanced Manufacturing Technology, 120(3), 2489-2501.

[11]. Rathore, S., Singh, R. K. R., Khan, K. L. A., (2021). Effect of process parameters on mechanical properties of aluminum composite foam developed by friction stir processing. Proceedings of the Institution of Mechanical Engineers. Part B: Journal of Engineering Manufacture. 235(12), 1892-1903.

[12]. Guan, R., Wang, Y., Zheng, S., Su, N., Ji, Z., Liu, Z., Chen, B., (2019). Fabrication of aluminum matrix composites reinforced with Ni-coated graphene nanosheets. Materials Science and Engineering: A. 754:437-446.

[13]. Taşcı, U., Yılmaz, T. A., Karakoç, H., Karabulut, Ş., (2024). Enhancing Wear Resistance and Mechanical Behaviors of AA7020 Alloys Using Hybrid Fe3O4-GNP Reinforcement. Lubricants. 12(6), 215.

[14]. Kurapova, O. Y., Smirnov, I. V., Solovyeva, E. N., Konakov, Y. V., Lomakina, T. E., Glukharev, A. G., Konakov, V. G., (2022). The Intermetallic Compounds Formation and Mechanical Properties of Composites in The Ni-Al System. Materials Physics & Mechanics. 48(1), 136-146.

[15]. Surappa, M. K., (2003). Aluminium matrix composites: Challenges and opportunities. Sadhana. 28(1-2), 319-334.

[16]. Abdel-Rahman, M., El-Sheikh, M. N., (1995). Workability in forging of powder metallurgy compacts. Journal of materials processing technology. 54(1-4), 97-102.

[17]. Tabandeh-Khorshid, M., Omrani, E., Menezes, P. L., Rohatgi, P. K., (2016). Tribological performance of self-lubricating aluminum matrix nanocomposites: role of graphene nanoplatelets. Engineering science and technology. an international journal, 19(1), 463-469.

[18]. Şenel, M. C., Gürbüz, M., Koç, E., (2019). Fabrication and characterization of aluminum hybrid composites reinforced with silicon nitride/graphene nanoplatelet binary particles. Journal of Composite Materials. 53(28-30), 4043-4054.

[19]. Gürbüz, M., Can Şenel, M., Koç, E., (2018). The effect of sintering time, temperature, and graphene addition on the hardness and microstructure of aluminum composites. Journal of Composite Materials. 52(4), 553-563.

[20]. Ghodrati, H., Ghomashchi, R., (2019). Effect of graphene dispersion and interfacial bonding on the mechanical properties of metal matrix composites: an overview. FlatChem. 16:100113.

[21]. Yang, S., Gao, X., Li, W., Dai, Y., Zhang, J., Zhang, X., Yue, H., (2024). Effects of the graphene content on mechanical properties and corrosion resistance of aluminum matrix composite. Journal of Materials Research and Technology. 28:1900-1906.